J|A|C|S
ARTICLES
Published on Web 08/06/2005

Magnetic and Porous Nanospheres from Ultrasonic Spray Pyrolysis

Won Hyuk Suh and Kenneth S. Suslick*

Contribution from the School of Chemical Sciences, University of Illinois at Urbana-Champaign, 600 South Mathews Avenue, Urbana, Illinois 61801

Received February 2, 2005; E-mail: ksuslick@uiuc.edu

Abstract: We have used an inexpensive high-frequency ultrasound generator from a household humidifier to create a useful source for ultrasonic spray pyrolysis and produced submicrometer silica particles that are porous on the nanometer scale. By using two heated zones, we first initiate polymerization of organic monomers in the presence of silica colloid, which creates *in situ* a composite of silica with an organic polymer, followed by a second heating to pyrolyze and remove the polymer. The morphology and surface area of the final porous silica are controlled by varying the silica-to-organic monomer ratio. In a single flow process, ferromagnetic cobalt nanoparticles can be easily encapsulated in the porous silica, and the resulting nanospheres are extremely resistant to air oxidation. Products were characterized by SEM, (S)TEM, EDS, XPS, and SQUID.

Introduction

Composite materials have played a critical role in technology for centuries, with the size of the components usually on the micrometer scale or above. Recent advances in nanotechnology have given us control over such materials in the submicrometer regime. For example, the preparation of metal, metal oxide, and semiconductor nanoparticles has been explored in some detail using a variety of approaches.[1,2] Aerosol methods are especially simple and scalable;[2] we report here the extension of ultrasonic spray pyrolysis (USP, Figure 1) as a simple, inexpensive, and versatile method for the multistep syntheses of nanocomposites in a continuous flow reactor, specifically porous inorganic oxide nanomaterials and silica-encapsulated metal nanoparticles.

High-intensity ultrasound is central to both USP and sonochemistry,[3] and both are proving useful for the synthesis of novel nanomaterials. Both use phase separation to create isolated reaction zones on the submicrometer scale. There is, however, a fundamental difference between the two: USP uses micrometer-sized liquid droplets isolated from one another in a hot gas, whereas sonochemistry uses micrometer-sized hot gas bubbles isolated in a cold liquid.[3]

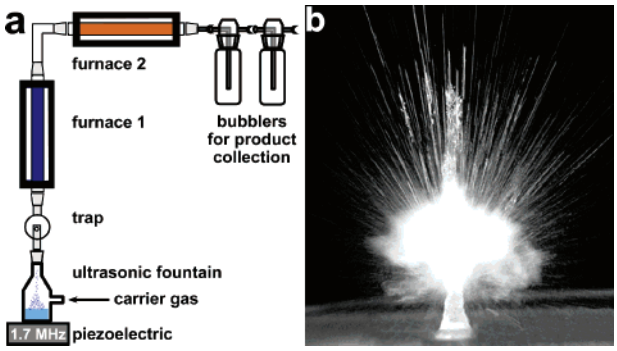

Figure 1. (a) Ultrasonic spray pyrolysis (USP) apparatus with dual furnaces. (b) Macrophotograph of an ultrasonic fountain and mist produced at 1.7 MHz (33-ms exposure, total width ~8 cm).

Spray pyrolysis,[2b−d] using a variety of methods to achieve precursor nebulization, offers a great flexibility in a continuous flow process for the synthesis of novel materials, potentially on a very large scale. Such materials include free nanoparticles and encapsulated nanoparticles in matrices (i.e., silica), porous materials. By tuning these characteristics of spray pyrolysis, various types of composite materials are made, and like the

(1) (a) Lu, Y.; Ran, H.; Stump, A.; Ward, T. L.; Rieker, T.; Brinker, C. J. *Nature* **1999**, *398*, 223−226. (b) Bonnemann, H.; Richards, R. M. *Eur. J. Inorg. Chem.* **2001**, 2455−2480. (c) Hyeon, T. *Chem. Commun.* **2003**, 927−934. (d) Alivisatos, P. *Nat. Biotechnol.* **2004**, *22*, 47−52. (e) Lee, S.-M.; Cho, S.-N.; Cheon, J. *Adv. Mater.* **2003**, *15*, 441−444. (f) Coe, S.; Woo, W.-K.; Bawendi, M.; Bulovic, V. *Nature* **2002**, *420*, 800−803. (g) Urban, J. J.; Yun, W. S.; Gu, Q.; Park, H. *J. Am. Chem. Soc.* **2002**, *124*, 1186−1187. (h) Xia, Y.; Yang, P. *Adv. Mater.* **2003**, *15*, 351. (i) Guo, W.; Li, J.; Wang, Y. A.; Peng, X. *J. Am. Chem. Soc.* **2003**, *125*, 3901. (j) Mirkin, C. A. *Inorg. Chem.* **2000**, *39*, 2258−2272. (k) Gudiksen, M. S.; Wang, J.; Lieber, C. M. *J. Phys. Chem. B* **2001**, *105*, 4062−4064. (l) Cushing, B. L.; Kolesnichenko, V. L.; O'Connor, C. J. *Chem. Rev.* **2004**, *104*, 3893−3946.

(2) (a) Lee, J.-H.; Park, S.-J. *J. Am. Ceram. Soc.* **1993**, *76*, 777−780. (b) Messing, G. L.; Zhang, S. C.; Jayanthi, G. V. *J. Am. Ceram. Soc.* **1993**, *76*, 2707−2726. (c) Patil, P. S. *Mater. Chem. Phys.* **1999**, *59*, 185−198. (d) Kodas, T. T.; Hampden-Smith, M. *Aerosol Processing of Materials*; Wiley-VCH: New York, 1999. (e) Xia, B.; Okuyama, K.; Lenggoro, I. W. *Adv. Mater.* **2001**, *13*, 1744−1744. (f) Kim, J. H.; Germer, T. A.; Mulholland, G. W.; Ehrman, S. H. *Adv. Mater.* **2002**, *14*, 518. (g) Okuyama, K.; Lenggoro, I. W. *Chem. Eng. Sci.* **2003**, *58*, 537−547. (h) Kozhukharov, V.; Brashkova, N.; Machkova, M.; Carda, J.; Ivanova, M. Ultrasonic spray pyrolysis for powder synthesis. In *Solid State Chemistry V*, Proceedings of the 5th International Conference on Solid State Chemistry, Bratislava, Slovakia, July 7-12, 2002; Sajgalík, P., Drábik, M., Varga, S., Eds.; Scitec Publications: Uetikon-Zurich, 2003; Vols. 90−91, pp 553−557.

(3) (a) Suslick, K. S.; Price, G. J. *Annu. Rev. Mater. Sci.* **1999**, *29*, 295. (b) McNamara, W. B., III; Didenko, Y.; Suslick, K. S. *Nature* **1999**, *401*, 772. (c) Crum, L. A.; Mason, T. J.; Reisse, J.; Suslick, K. S., Eds. *Sonochemistry and Sonoluminescence*; NATO ASI Series C; Kluwer Publishers: Dordrecht, The Netherlands, 1999; Vol. 524. (d) Flannigan, D. J.; Suslick, K. S. *Nature* **2005**, *434*, 52−55. (e) Dhas, N. A.; Suslick, K. S. *J. Am. Chem. Soc.* **2005**, *127*, 2368−2369.

solution method (i.e., hydrothermal) metal, metal oxide, and semiconductor particles have been synthesized.[2,4] More specifically, interesting magnetic and porous nanomaterials previously prepared by various forms of spray pyrolysis include the synthesis of Fe_2O_3,[4a] $NiFe_2O_4$,[4b] ZrO_2,[4c] SiO_2,[1a,4d,e] Al_2O_3,[4f] TiO_2,[4g] cobalt-doped TiO_2,[4h] Ni,[4i] NiZn,[4j] Co,[4k] Pt/Al_2O_3,[2b] Pt/SiO_2,[4l] $Fe_2O_3-SiO_2$,[4m] FeCo/MWNT,[4n] Fe/MgO,[4o] and $BaFe_{12}O_{19}$.[4p] Other examples can be found in review articles.[1l,2b−d,g,h]

Experimental Section

General Methods. All chemicals were handled under nitrogen or argon and are available commercially. Silica colloid LUDOX HS-40, styrene, ethylene glycol dimethacrylate, AIBN, SDS, and nanoparticle Co_3O_4 were purchased from Aldrich Chemicals. Dicobalt octacarbonyl was purchased from Strem. 1,4-Dioxane was purchased from Fisher Scientific. Water was purified and filtered using a Barnsted Nanopure system.

Typical Experiment Condition. Silica colloid (LUDOX HS-40, 12-nm diameter) (1 mL), styrene (2 mL), ethylene glycol dimethacrylate (1.6 mL), AIBN (16.4 mg), $Co_2(CO)_8$ (0.15 g), 1,4-dioxane (30 mL), and 0.01 M SDS in purified water (75 mL) were mixed and nebulized. The first furnace was 200 °C, and the second 700 °C. The flow rate of inert gas (N_2 or Ar) was typically 1 SLPM; the residence time through the furnaces is controlled by the gas flow rate and is typically a few seconds. For nebulization, a Sunbeam model 696, 1.7 MHz household ultrasonic humidifier (<$30) was used (Figure 1). After 6 h of collection into water-filled bubblers, the black magnetic colloidal particles were isolated by centrifugation at 10 000 rpm. Typical yield is ~40%. The products were washed with purified water at least three times, re-isolated by centrifugation, and sampled for analysis.

Characterization. SEM measurements were taken on a Hitachi S-4700, TEM measurements were taken on a JEOL 2010-F, XPS measurements were taken on a Physical Electronics PHI 5400 X-ray photoelectron spectrometer, and magnetic measurements were taken on 1T and 7T MPMS SQUID magnetometer.

Results and Discussion

We nebulize a precursor solution using the ultrasonic transducer from a commercially available household ultrasonic humidifier (1.7 MHz) into a quartz tube inside two furnaces in series (Figure 1a). The nebulization process is due to the formation of an ultrasonic fountain from the high-frequency ultrasound (as shown in Figures 1b and 2).

In this study, an aqueous precursor solution was used that contained polymerizable organic monomers with a radical initiator, colloidal silica nanoparticles, and surfactant; in some cases, a small amount of $Co_2(CO)_8$ was also added to produce magnetic nanospheres. The solution was nebulized into an inert gas stream that carried the resulting droplets into the first furnace (200 °C), where the solvent evaporated and the organic monomer polymerized forming an inorganic−organic nanocomposite. The resulting particles were carried into a second, hotter furnace

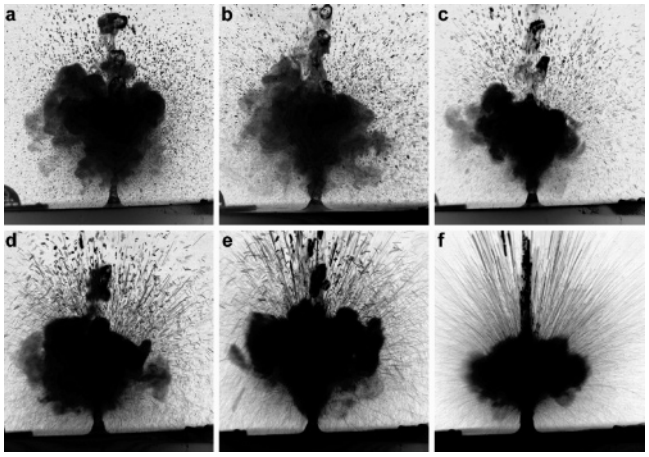

Figure 2. Photographs of the ultrasonic fountain as a function of shutter speed with water as solvent. For improved contrast, the negative image is shown. The estimated velocity of the fast moving larger droplets is ~5 m/s. SONY DSC-F828 digital camera: (a) 0.5, (b) 1, (c) 2, (d) 4, (e) 8, and (f) 16 ms. Each photograph is ~15 × 15 cm^2.

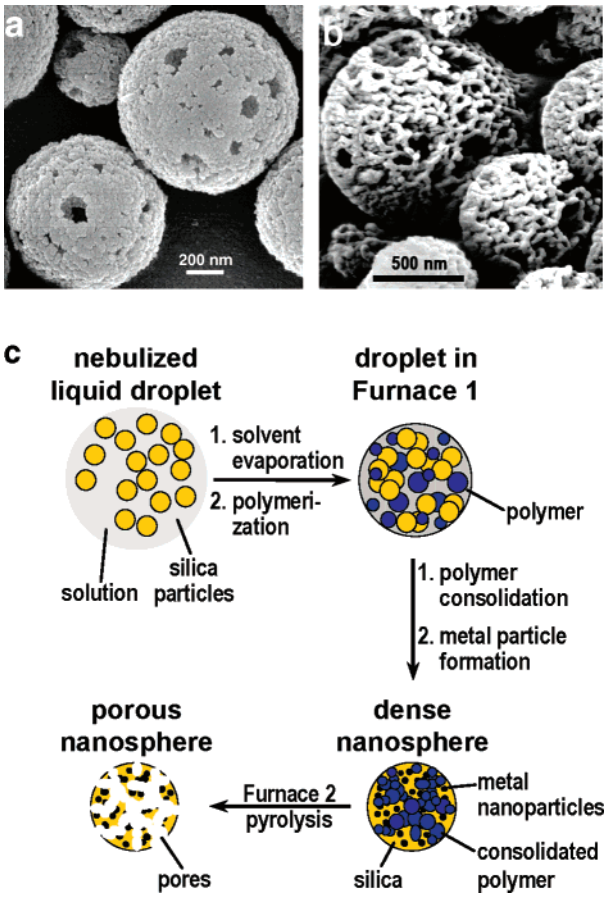

Figure 3. (a) SEM of nanospheres produced by USP of solutions with 3:1 w/w monomer/silica; 1.2% $Co_2(CO)_8$ also present. The silica colloid particle size was 12 nm. (b) Inner structure of particle a is shown after sputtering. A wormlike microstructure is clearly shown. (c) Schematic representation of the multistage process of porous silica nanosphere formation.

(4) (a) Martinez, B.; Roig, A.; Molins, E.; Gonzalez-Carreno, T.; Serna, C. J. *J. Appl. Phys.* **1998**, *83*, 3256−3262. (b) Chung, Y. S.; Park, S. B.; Kang, D.-W. *Mater. Chem. Phys.* **2004**, *86*, 375−381. (c) Zhang, S. C.; Mulholland, G.; Messing, G. L. *J. Mater. Synth. Process.* **1996**, *4*, 227−233. (d) Iskandar, F.; Mikrajuddin; Okuyama, K. *Nano Lett.* **2002**, *2*, 389−392. (e) Fan, H.; Swol, F. V.; Lu, Y.; Brinker, C. J. *J. Non-Cryst. Solids* **2001**, *285*, 71−78. (f) Kim, S. H.; Liu, B. Y. H.; Zachariah, M. R. *Chem. Mater.* **2002**, *14*, 2889−2899. (g) Jokanovic, V.; Spasic, A. M.; Uskokovic, D. *J. Colloid Interface Sci.* **2004**, *278*, 342−352. (h) Manivannan, A.; Seehra, M. S.; Majumder, S. B.; Katiyar, R. S. *Appl. Phys. Lett.* **2003**, *83*, 111−113. (i) Xia, B.; Lenggoro, W.; Okuyama, K. *J. Mater. Sci.* **2001**, *36*, 1701−1705. (j) Nam, J.-H.; Kim, W. K.; Park, S. J.; Yeo, D.-H.; Kim, H. T. *Phys. Status Solidi A* **2004**, *201*, 1846−1850. (k) Jang, H. D.; Hwang, D. W.; Kim, D. P.; Kim, H. C.; Lee, B. Y.; Jeong, I. B. *Mater. Res. Bull.* **2004**, *39*, 63−70. (l) Bore, M. T.; Ward, T. L.; Fukuoka, A.; Datye, A. K. *Catal. Lett.* **2004**, *98*, 167−172. (m) Tartaj, P.; Gonzalez-Carreno, T.; Serna, C. J. *Adv. Mater.* **2001**, *13*, 1620−1624. (n) Elias, A. L.; Rodriguez-Manzo, J. A.; McCartney, M. R.; Golberg, D.; Zamudio, A.; Baltazar, S. E.; Lopez-Urias, F.; Munoz-Sandoval, E.; Gu, L.; Tang, C. C.; Smith, D. J.; Bando, Y.; Terrones, H.; Terrones, M. *Nano Lett.* **2005**, *5*, 467−572. (o) Choa, Y.-H.; Yang, J.-K.; Kim, B.-H.; Jeong, Y.-K.; Lee, J.-S.; Nakayama, T.; Sekino, T.; Niihara, K. *J. Magn. Magn. Mater.* **2003**, *266*, 12−19. (p) Tang, Z. X.; Nafis, S.; Sorensen, C. M.; Hadjipanayis, G. C.; Klabunde, K. J. *IEEE Trans. Magn.* **1989**, *25*, 4236−4238.

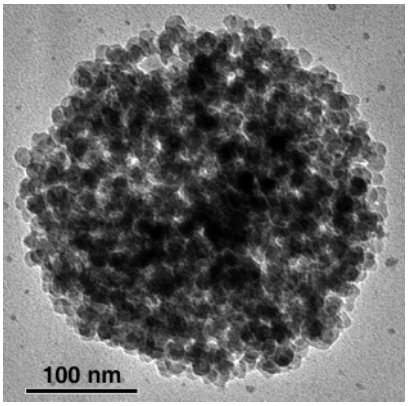

Figure 4. TEM image of cobalt-doped porous silica nanosphere prepared from 3:1 organic monomer/silica (i.e., same material as that in Figure 3a). On close inspection, Co nanoparticles can be observed embedded on the silica nanoparticles that make up the porous sphere.

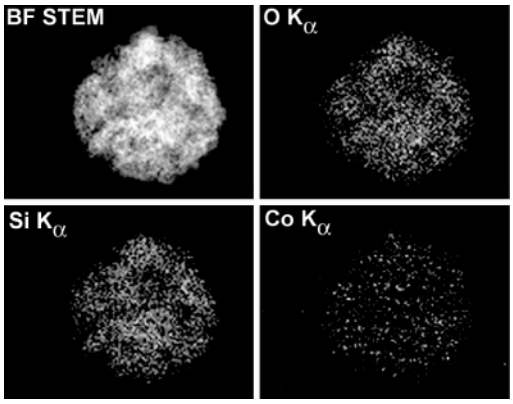

Figure 5. STEM EDS analysis of cobalt-doped porous silica prepared from 10:1 organic monomer/silica (i.e., same material as that in Supporting Information Figure 2b) shows an even distribution of Co throughout the entire particle.

(700 °C) where the organic polymer was fully pyrolyzed, leaving behind porous silica nanospheres (Figure 3). The nanospheres were collected in a water-filled bubbler as an aqueous colloidal solution and subsequently isolated by centrifugation. The products of the pyrolysis of the polymer form a small amount of an orange tar, which is soluble only in organic solvents, contains primarily phenyl groups (by NMR, Supporting Information Figure 2), and is blue-green luminescent under UV light.

The morphology, size distribution, and composition of the silica nanospheres were analyzed using SEM, TEM, STEM, and EDS. The size distribution of the isolated nanospheres was 800 nm (±400 nm, $N > 500$, Supporting Information Figure 3a). Some of this polydispersity is due to droplet coalescence in the high-density mist (Figure 1b and 2) and may be improved by higher velocity gas flow with longer tube furnaces to provide equivalent residence times.[2,4]

The morphology and surface area of the resulting nanospheres are controlled by the ratio of organic monomers to colloidal silica (Figure 3 and Supporting Information Figure 3). When the monomer-to-silica ratio was 3:1 w/w, the resulting porous nanoparticles had a surface area of 120 m^2/g, as determined by standard BET N_2 adsorption (Figure 3a). For comparison, when the ratio was 10:1, the surface was 80 m^2/g, and more macropores were generated (Supporting Information Figure 3b). Increasing the monomer to silica further prevents formation of sphere formation, presumably due to limited structural integrity after pyrolysis of the organic phase (Supporting Information Figure 3d).

TEM (Figure 4) and STEM (Figure 5) images further illustrate the pores created from the pyrolysis of the organic polymer initially formed in the consolidation process. Pre-existing polystyrene beads have been previously used for similar purposes.[4d] The advantage of our method of *in situ* polymerization is simply that of expense and convenience. In addition, we can add a third component to the system. For example, the inclusion of Co nanoparticles within the porous silica nanospheres was easily accomplished by the addition of $Co_2(CO)_8$ to the initial precursor solution.

Using EDS line analysis (which probes the entire depth of the nanosphere[5]) at nanometer resolution, we were able to detect Si K_α, O K_α, and Co K_α signals, verifying the presence of SiO_2 and Co(0) (Supporting Information Figure 4). EDS quantitative analysis (TEM) revealed that the amount of cobalt encapsulated was between 1.2 and 2.3%.

XPS analysis (which is sensitive only to surface composition), however, could barely detect any Co 2p signal (Supporting Information Figure 5). This indicates that during the consolidation process, the cobalt nanoparticles were mostly encapsulated inside the porous silica spheres. XPS depth profile analysis revealed the presence of cobalt inside the sphere after sputtering, confirming its presence as encapsulated nanoparticles. Furthermore, the binding energy was 779.4 eV, indicating that cobalt is in its metallic state (zero). In comparison, Co 2p in the Aldrich Co_3O_4 nanoparticle sample was 780.6 eV, while the metallic cobalt sample was 780.1 eV. These data are consistent with

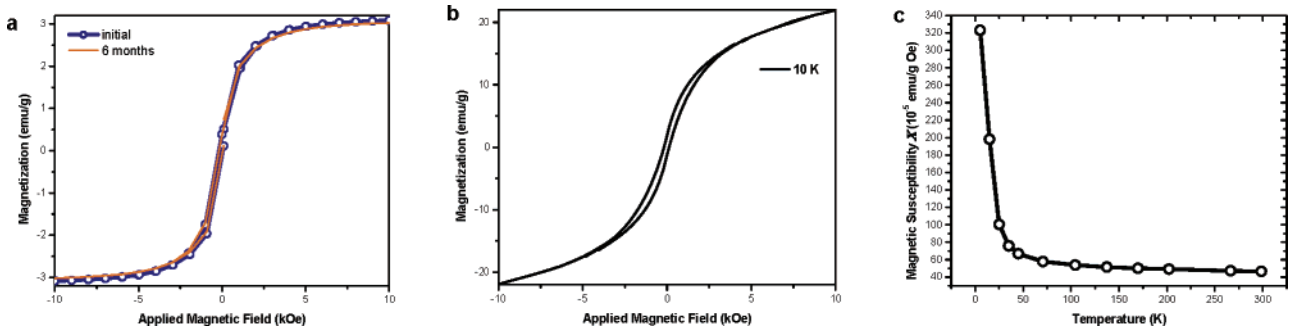

Figure 6. Magnetic response of cobalt-doped porous silica nanospheres prepared from 10:1 organic monomer/silica (i.e., the same material as that in Supporting Information Figure 2a). (a) Excellent air stability is observed, even after 6 months. Magnetization vs applied magnetic field at 298 K. (b) At 10 K, hysteresis loop is clearly observed which confirms the presence of ferromagnetic cobalt species. (c) Temperature variation of the magnetic susceptibility at $H = 5000$ Oe.

literature values.[5b] In the XPS data, the presence of C1s peak is due to the background signal.

SQUID magnetic susceptibility measurements (Figure 6) confirmed the presence of ferromagnetic Co(0) nanoparticles. The stability of the encapsulated Co(0) nanoparticles to air oxidation was excellent: the ferromagnetic hysteresis curve is nearly identical even after 6 months of storage in air, consistent with a complete silica encapsulation of the Co nanoparticles. Last, comparing the saturation magnetization signal (emu/g) of the silica nanocomposite (3 emu/g for the 10:1 organic monomer/silica sample, Figure 6a) with 100% metallic cobalt (143 emu/g, Supporting Information Figure 6), our cobalt-doped porous silica sample should contain approximately 2% metallic cobalt, which corresponds nicely with EDS quantitative analysis data (2.3% Co).

Conclusions

In conclusion, our studies have shown that the use of an inexpensive high frequency ultrasound generator from a household humidifier allows the creation of nanocomposite materials composed of metal nanoparticles and metal oxide matrix. Using a USP setup with two separately heating zones, we have produced submicrometer silica particles, porous on the nanometer scale. Pores were created *in situ* after initial synthesis of a silica/organic polymer composite, followed by a second heating to pyrolyze and remove the polymer. By varying the silica-to-organic monomer ratio, morphology and surface area of the final porous silica can be controlled. In addition, in a single flow process, ferromagnetic cobalt nanoparticles can be easily encapsulated in the porous silica. Magnetization studies have shown that the resulting nanospheres are extremely resistant to air oxidation.

Acknowledgment. We thank Dr. Yuri Didenko for helpful discussions. This work was supported by the National Science Foundation (CHE-03-15494). Analysis was carried out at the Center for Microanalysis of Materials (DEFG02-91ER45439) and the Frederick Seitz Materials Research Laboratory (DEFG02-91-ER45439) at the University of Illinois at Urbana-Champaign.

Supporting Information Available: SEM, (S)TEM, XPS data, and macrophotographs of the ultrasonic fountain. This material is available free of charge via the Internet at http://pubs.acs.org.

JA050693P

(5) (a) Goodhew, P. J.; Humphreys, J.; Beanland, R. *Electron Microscopy and Analysis*; Taylor & Francis: London and New York, 2001. (b) Watts, J. F.; Wolstenholme, J. *An Introduction to Surface Analysis by XPS and AES*; Wiley: London, 2003.